The MR appearance of gray and white matter in the cervical spinal cord.

L F Czervionke, D L Daniels, P S Ho, S W Yu, P Pech, J A Strandt, A L Williams and V M Haughton

AJNR Am J Neuroradiol 1988, 9 (3) 557-562
http://www.ajnr.org/content/9/3/557

The MR Appearance of Gray and White Matter in the Cervical Spinal Cord

Leo F. Czervionke[1]
David L. Daniels
Peter S. P. Ho
Shiwei Yu
Peter Pech[2]
Julie A. Strandt
Alan L. Williams
Victor M. Haughton

Artifacts that can distort the appearance of the cervical spinal cord are caused by data truncation during MR image reconstruction. We used a phantom and then correlated anatomic sections with MR images in cadavers and normal volunteers to evaluate the effect of truncation artifacts on the MR appearance of the spinal cord. When truncation artifacts are minimized, the gray matter and major white-matter columns in the cervical cord can be recognized. T2-weighted gradient-echo MR techniques can best differentiate gray from white matter.

Artifacts that can alter the MR appearance of cervical spine images include those produced by data truncation, patient motion, vascular and CSF pulsation, chemical shift, even-echo rephasing, and magnetic field distortions [1–4]. The concept of the truncation artifact (Gibb phenomenon) in MR is not new, but the effect of truncation artifacts on the appearance of the cervical spinal cord has not been analyzed [5–7]. Our purpose is to describe the MR appearance of the cervical cord gray and white matter and to demonstrate the effect of truncation artifacts on the MR appearance.

Materials and Methods

A phantom containing test tubes was designed to simulate the shape of the spinal cord. Three test tubes with diameters of 10, 13, and 16 mm were filled with a saline solution. A fourth test tube measuring 13 mm in diameter was filled with corn oil. The fifth tube contained air and measured 13 mm in diameter. All test tubes were suspended in a gelatin-containing saline solution. Spin- and gradient-echo MR images of the phantom were obtained. With the phase-encoding axis set perpendicular to the long axis of the test tubes, the following parameters were used: TR = 2000, TE = 20, one excitation, 128 × 256 and 256 × 256 matrix, 5-mm slice thickness, and 20- and 24-cm field of view.

Seven normal volunteers and three fresh cadavers were examined on a 1.5-T MR scanner* with a combination of spin-echo and gradient-echo pulse sequences. The MR images were compared with sagittal and axial MR scans obtained in the three cadavers. Anatomic sections in the cadavers were obtained by cryomicrotome techniques previously described [8] and were compared with the MR images. A 3-in. butterfly surface coil was used to examine the cadavers and volunteers.

T1- and T2-weighted MR images were obtained. Image parameters used to obtain T1-weighted spin-echo (SE) images included TR = 800, TE = 20, two or four excitations, 128 × 256 or 256 × 256 matrix, 3- or 5-mm slice thickness, and 16-, 20-, or 24-cm field of view. Proton-density and T2-weighted SE images were obtained in conjunction with ECG or peripheral gating with TR = 2000–2500, TE = 20 and 80, one excitation, 128 × 256 or 256 × 256 matrix, 5-mm slice thickness, and 20- or 24-cm field of view.

Two types of gradient-echo MR techniques were used. (1) GRE is a sequential single-slice technique that was used in conjunction with gradient moment-nulling flow compensation. T2-weighted GRE were acquired with the following parameters: TR = 200, TE = 13, four excitations, 128 × 128 or 256 × 256 matrix, 24-cm field of view, and 10° flip angle. T1-

* GE Medical Systems, Milwaukee, WI.

Received May 15, 1987; accepted after revision October 19,1987.

[1] All authors: Department of Radiology, Medical College of Wisconsin, Froedtert Memorial Lutheran Hospital, 9200 W. Wisconsin Ave., Milwaukee, WI 53226. Address reprint requests to L. F. Czervionke.

[2] Present address: Department of Radiology, University Hospital, S-750 14 Uppsala, Sweden.

***AJNR* 9:557–562, May/June 1988**
0195–6108/88/0903–0557

weighted GRE pulse sequences were not obtained. (2) PSI is a true multislice gradient-echo technique. Cardiac gating was not used with the PSI pulse sequences. T1-weighted PSI images were acquired with TR = 300–500, TE = 8–10, one or two excitations, 128 × 256 or 256 × 256 matrix, 3- or 5-mm slice thickness, 20- or 24-cm field of view, and 120° flip angle. Proton-density and T2-weighted PSI images were obtained with TR = 750, TE = 8–10 and 18–20, two excitations, 256 × 256 matrix, 3- or 5-mm slice thickness, 20- or 24-cm field of view, and 10° flip angle.

Results

The test tube phantom study characterized truncation artifacts. In the axial or sagittal plane these artifacts were seen as alternating bands of low and high signal intensity parallel to the wall of each test tube. These bands are propagated along the phase-encoding axis, but they are oriented perpendicular to this axis. They were more conspicuous in the phase-encoding direction when a 128 × 256 matrix was used. They were less evident when a 256 × 256 matrix was used (Fig. 1). In axial images, these bands had a slightly oval shape with the long axis of the artifact perpendicular to the phase-encoding axis. The number of truncation bands within the tubes increased with increasing tube diameter. The 10-mm-diameter test tube (which most closely corresponds to the normal spinal cord diameter) contained a prominent, centrally located band in both the axial and sagittal planes.

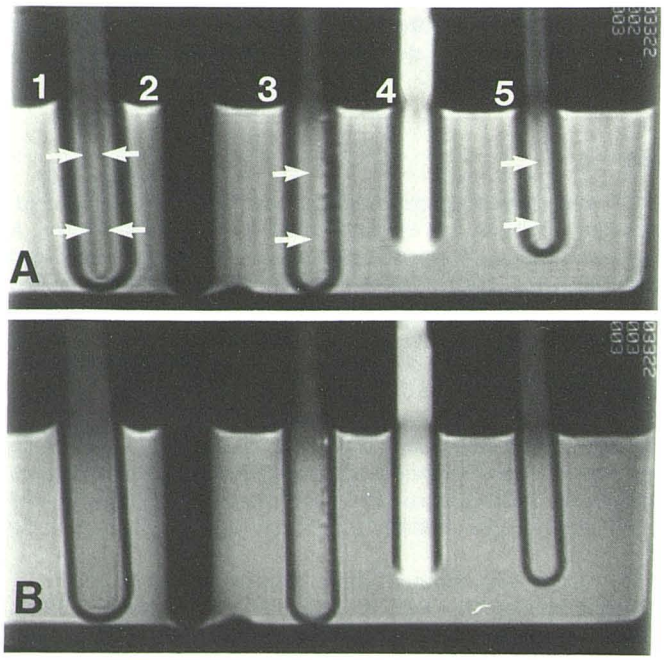

Fig. 1.—Test tube phantom showing effects of truncation artifacts at 24-cm field of view. Test tubes 1, 3, and 5 contain saline. Test tubes 2 and 4 contain air and oil, respectively. In row A, 128 × 256 matrix was used; in row B, 256 × 256 matrix was used (phase-encoding axis right-left). Truncation artifacts are seen as alternating bands of low and high signal intensity parallel to test tube walls. Truncation artifacts are negligible in row B but are not eliminated, even with a 256 × 256 matrix. Note that there are more truncation bands in tube 1 (16-mm diameter) than in tube 5 (10-mm diameter). Tube 5 contains a single truncation band and more closely approximates normal spinal cord diameter.

On sagittal proton-density and T2-weighted spin- or gradient-echo MR images obtained in cadavers with a 256 × 256 matrix, the prominent structure observed within the cord is a thin band of high signal intensity located in the cord anterior to midline. This band corresponds in location and width to central gray matter seen on sagittal anatomic sections (Fig. 2). This band of gray matter extended into the posterior aspect of the medulla and terminated at the obex.

Another type of band was seen in sagittal MR images with a 128 × 256 matrix. It was broader than the true central gray-matter band and located midline in the cord. With both spin- and gradient-echo techniques, this band had low signal intensity on T1-weighted images and high signal intensity on proton-density-weighted and T2-weighted images. When matrix size was changed to 256 × 256, this midline band was no longer obvious: In the T1-weighted images, the cord appeared homogeneous (Fig. 3); in the T2-weighted images, the thin band of bright signal corresponding to central gray matter became apparent, located anterior to the midline of the cord (Fig. 4).

On axial T2- and proton-density-weighted MR images obtained with a 256 × 256 matrix in cadavers, the cervical gray matter had higher signal intensity than the white matter. The configuration of gray and white matter correlated with anatomic sections (Fig. 5). This same appearance was also observed in axial proton-density-weighted and T2-weighted spin-echo and gradient-echo MR images obtained in normal volunteers (Fig. 6). In T1-weighted axial images, a pattern was seen that correlated less exactly with the gray and white matter distribution seen on T2-weighted images. In the midline, a hypointense, triangular-shaped structure was noted posteriorly and this was flanked by small, round, hypointense structures in the lateral aspect of the cord (Fig. 6A). Portions of the cord white matter were isointense with gray matter.

Discussion

Without the artifacts caused by pulsatile CSF, flowing blood, and patient motion, the MR images from cadavers demonstrated the gray and white matter in the cervical spinal cord effectively. Because of postmortem changes, MR images in cadavers were not anticipated to be identical to those in live humans. Nevertheless, the images were qualitatively similar.

The phantom is not an ideal model for studying the interface between cord and CSF because the test tube walls have thickness. However, the phantom study did predict the truncation effects observed in MR images of normal volunteers and how the artifact may be minimized to reveal normal gray matter within the cord.

Data truncation artifacts (Gibb phenomenon) occur at high contrast interfaces (e.g., between cord and CSF) when Fourier transforms are used to reconstruct images from acquired MR data [1–3]. Because only a finite amount of phase and frequency information is obtained and stored in the data matrix, the Fourier series used to transform these data into images is finite—that is, "truncated."

Image reconstruction using finite (truncated) Fourier series

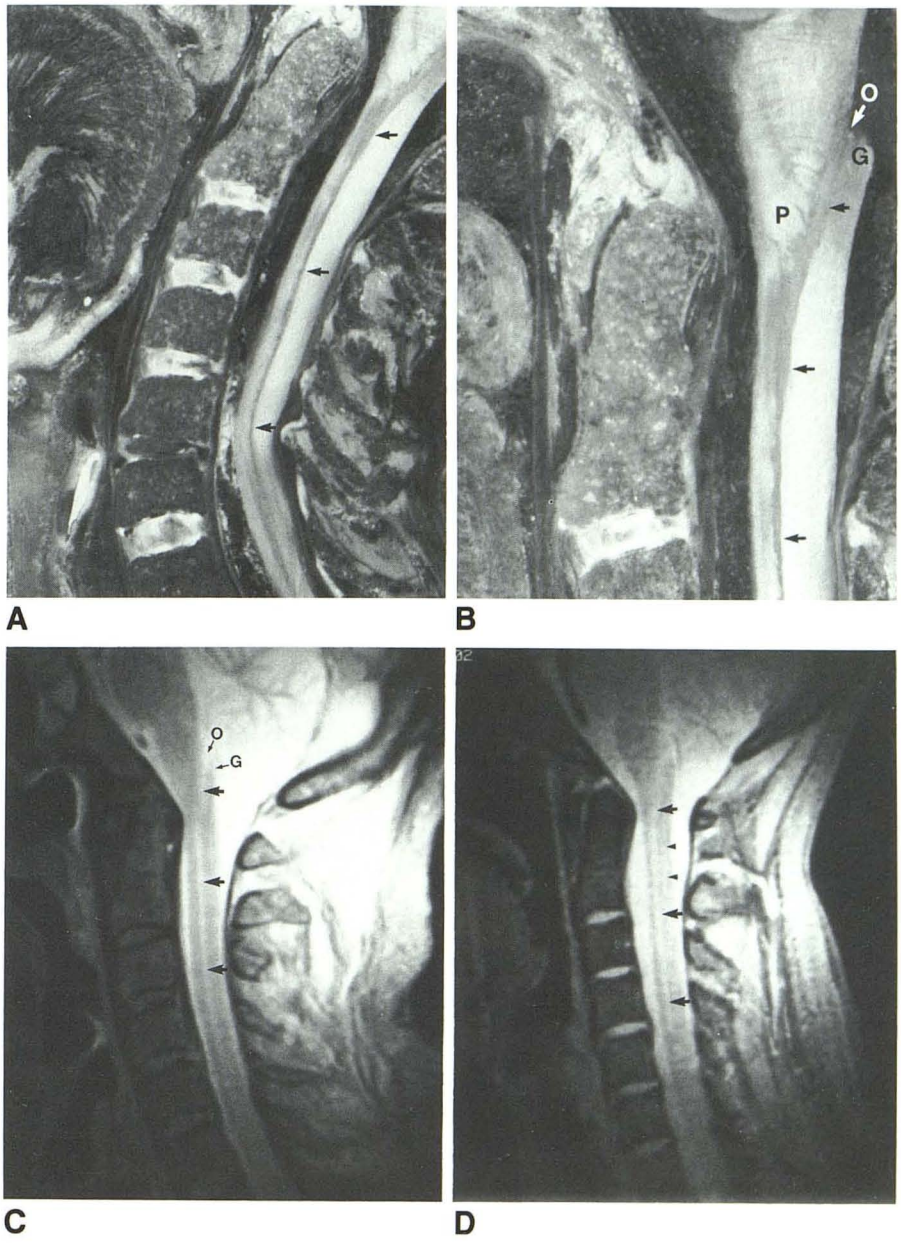

Fig. 2.—Sagittal cervical spine.

***A*, Anatomic section shows that most of the gray matter (*arrows*) is located anterior to cord midline.**

***B*, Anatomic section at cervicomedullary junction shows that central gray matter (*arrows*) is positioned posterior to decussating pyramidal tracts (P) extending toward obex (O). G = gracilis tubercle.**

***C*, Proton-density-weighted MR image in cadaver shows central gray matter in cord located slightly anterior to midline (*arrows*) (27-min acquisition time).**

***D*, Proton-density-weighted gradient-echo image in normal volunteer shows same position of central gray matter (*arrows*) (3-min acquisition time). Note that a thin, faint, white truncation band still occurs in cord posterior to midline (*arrowheads*), even with a 256 × 256 matrix.**

results in imprecise depiction of boundaries or interfaces where there is an abrupt transition between zones of high and low signal intensity. In MR images, this impression is represented by truncation artifacts that appear as alternating bands of high and low signal intensity, which parallel high-contrast interfaces and become less conspicuous with increasing distance from the interface. Mathematically, truncation artifacts are represented by an oscillating function that resembles a sine wave, except its peaks and valleys (maxima and minima) diminish in amplitude with increasing distance from the interface [9].

The peaks and valleys of this oscillating "sinc" function alternately "overshoot" and "undershoot" the true signal intensity of tissue on both sides of the interface and correspond to the truncation bands seen on MR images.

When two high-contrast interfaces are in proximity (e.g., anterior and posterior cord/CSF boundary), truncation artifacts produced at each interface will cancel or reinforce one another depending on the distance between the interfaces (Czervionke L, unpublished data). Therefore, the number and intensity of truncation bands seen between two interfaces depend on the distance between the interfaces (Fig. 1).

With a 24-cm field of view and 128 × 256 matrix, a dark truncation band is seen within the spinal cord on T1-weighted images because the CSF has low signal intensity at the cord interface (Fig. 3A). With a 256 × 256 matrix, the truncation artifact is less conspicuous (Figs. 1 and 3B). On T2-weighted MR images in which the CSF has high signal intensity, a bright, single, broad truncation band is seen centrally in the cord when a 128 × 256 matrix is used (Fig. 4A). When the

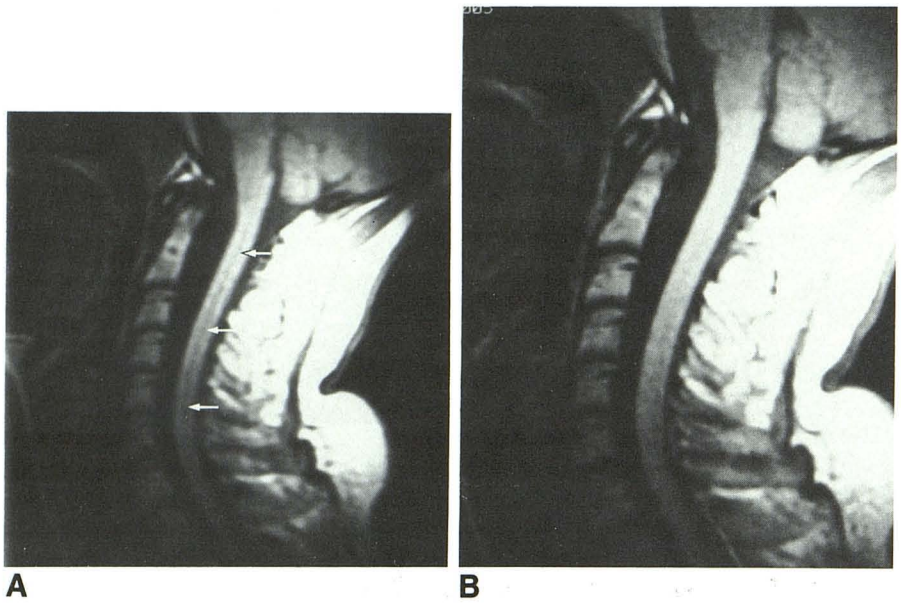

Fig. 3.—Sagittal spin-echo T1-weighted MR images of cervical spine in normal volunteer obtained with identical scan parameters except that a 128 × 256 matrix was used in *A* (phase-encoding axis is anterior-posterior) and a 256 × 256 matrix was used in *B*. Note band of low signal intensity (*arrows* in *A*) disappears in *B*. In *A*, the dark band within cord is caused predominantly by truncation artifact. Field of view is 24 cm in *A* and *B*.

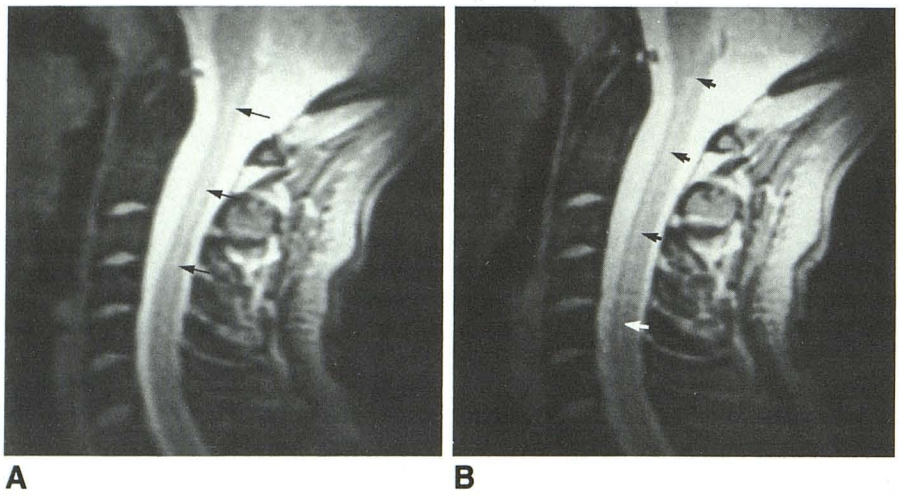

Fig. 4.—Sagittal gradient-echo T2-weighted MR images of cervical spine in normal volunteer obtained with identical parameters except that a 128 × 256 matrix was used in *A*, and a 256 × 256 matrix was used in *B* (phase-encoding axis is anterior-posterior). In *A*, a broad, high-signal-intensity truncation band is seen within cord in midline. In *B*, this bright truncation band has disappeared, leaving only a thin strip of high signal intensity located in cord anterior to midline, which corresponds to central gray matter. Field of view is 24 cm in *A* and *B*.

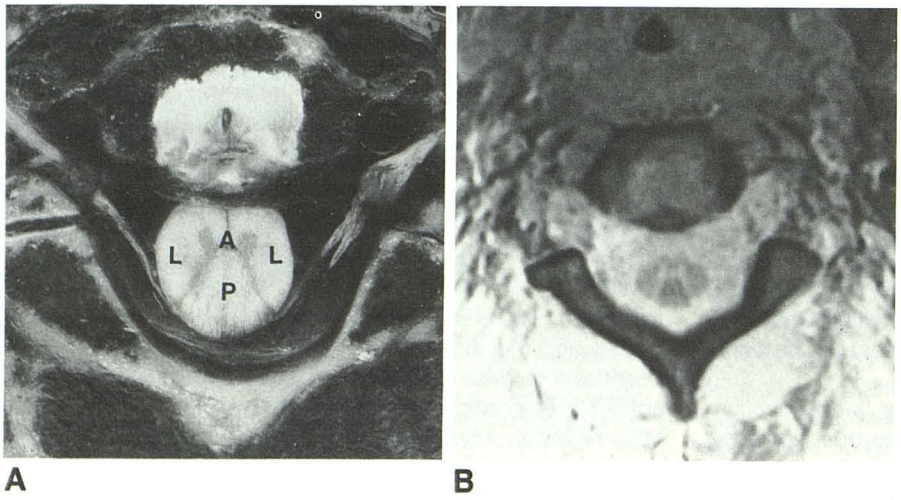

Fig. 5.—Axial cervical spine, C2–C3 level.

A, Anatomic section shows cord containing butterfly configuration of gray matter and adjacent white-matter columns (A = anterior, L = lateral, P = posterior white-matter columns). Note small, bulbous configuration of anterior horns.

B, Proton-density-weighted MR image in cadaver at same level shows similar configuration of gray and white matter in cord (27-min acquisition).

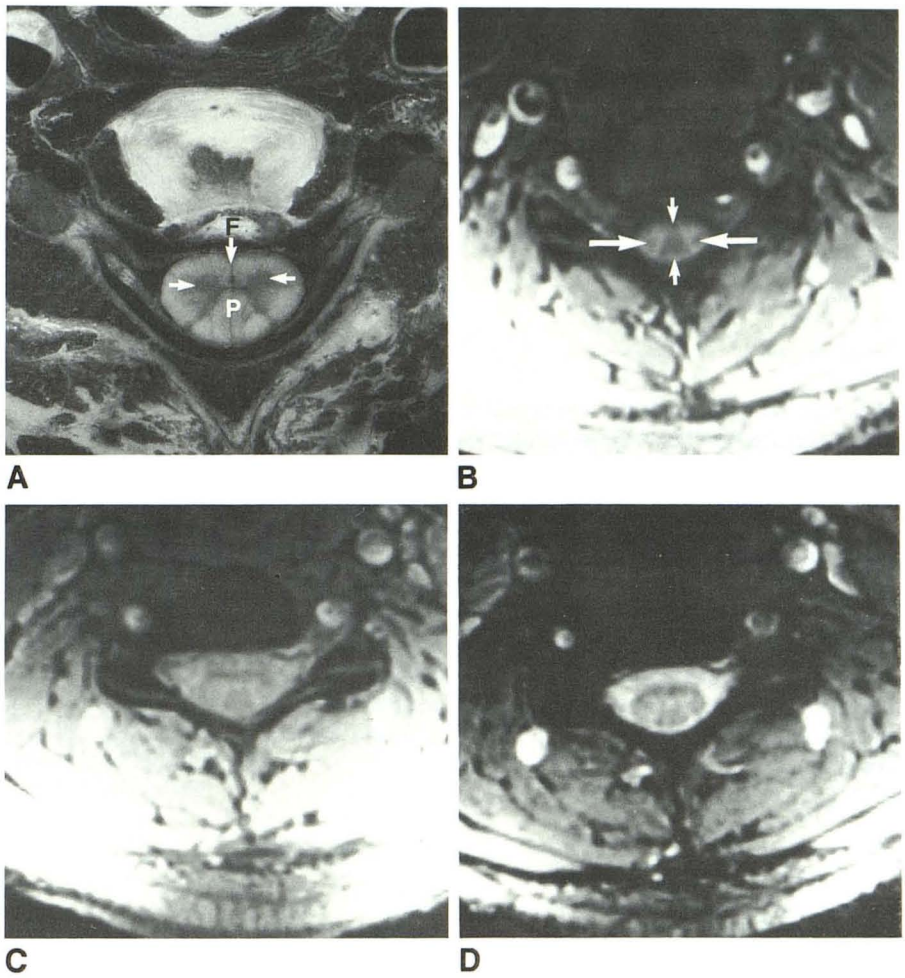

Fig. 6.—Axial cervical spine, C5–C6 level.

***A*, Anatomic section shows that posterior column (P) has triangular shape. F = anterior median fissure. Note anterior horns (*arrows*) are larger at this level.**

***B*, Axial T1-weighted gradient-echo image in normal volunteer. TR = 450, TE = 8. Note triangular region of low intensity (*small arrows*) in cord corresponds approximately to posterior white-matter columns. Anterior portion of "triangle" points toward anterior median fissure. Small round structures in cord laterally (*large arrows*) correspond to position of lateral corticospinal tracts.**

***C* and *D*, In same volunteer, proton-density-weighted (*C*) and T2-weighted gradient-echo image (*D*) reveal butterfly configuration of gray matter and adjacent white matter. TR = 750, TE = 9 and 18.**

truncation artifact is minimized by using a 256 × 256 matrix, the thin bright band of central gray matter in the anterior aspect of the cord can be demonstrated (Figs. 4B and 2D). However, even by increasing the matrix size to 256 × 256, the truncation artifact is not completely eliminated (see Fig. 1). For example, a 256 × 256 matrix was used to obtain Fig. 2D. In this figure, a thin, faint white band appears in the cord posterior to midline, which represents a truncation band. Truncation bands are particularly well seen on sagittal MR images in the cord because the highly contrasting CSF/cord interfaces, anteriorly and posteriorly, remain relatively equidistant throughout the cervical spine.

Gradient-echo MR techniques effectively demonstrate the gray matter and adjacent white-matter columns of the cervical cord in the clinical setting where relatively short acquisition times are preferable. Gradient-echo images provide greater tissue contrast than do spin-echo images for a given acquisition time [10]. With long acquisition times, similar contrast between gray and white matter can be achieved with spin-echo pulse sequences (Figs. 2C and 5B).

The majority of the cervical cord gray matter is located in the anterior aspect of the cord on either side of the central canal, and this gray matter can be demonstrated on axial and sagittal MR. More cephalad, the bulk of the gray matter accompanies the central canal into the posterior medulla toward the obex.

On axial anatomic sections, the anterior and posterior horns are thin structures in the upper cervical cord, but the anterior horns widen and progress caudally toward the cervical enlargement (Figs. 5 and 6). The butterfly configuration of the cord gray matter can be seen on axial MR images.

Relative to white matter, gray matter in the cord or brain has longer T2 and therefore displays higher signal intensity than white matter on T2-weighted images. The T1 relationship of gray and white matter in the cord is not the same as that observed in the brain. In the brain, the T1 of gray matter exceeds that of white matter; in the cord, some white-matter tracts clearly have longer T1 than does gray matter, while portions of the white matter are nearly isointense with gray matter. This was observed on T1-weighted spin-echo and gradient-echo images. For example, on T1-weighted axial MR images (Fig. 6B), the triangular-shaped region of low intensity

posteriorly conforms to a large portion of the posterior columns. Similarly, small round areas of low intensity in the lateral aspects of the cord do not correspond to the full extent of the lateral white-matter columns. Anatomically, these round regions correlate with the location of the lateral corticospinal tracts [11]. Further work is needed to determine why some white-matter tracts have different signal intensity than others and why some cord white matter appears to have longer T1 than does cord gray matter.

Conclusion

The central gray matter of the spinal cord is best seen on proton-density and T2-weighted gradient-echo axial or sagittal images when a 256 × 256 matrix is used. The gray matter may also be seen on T1- or T2-weighted spin-echo images if long acquisition times are attained. When using a 128 × 256 matrix, truncation artifacts produce distortion of the central gray matter in axial and sagittal images. Truncation artifacts in the cord are seen best on sagittal images, where they may be mistaken for syringohydromyelia. Therefore, a 256 × 256 matrix is recommended in cervical spine MR imaging. The ability to recognize the central gray matter and adjacent white matter with MR should prove helpful in diagnosing cervical cord disease.

REFERENCES

1. Wood ML, Henkelman RM. Truncation artifacts in magnetic resonance imaging. *Magn Reson Med* **1985**;2:517–526
2. Lufkin RB, Pusey E, Stark DD, Brown R, Leikind B, Hanafee WN. Boundary artifacts due to truncation errors in MR imaging. *AJR* **1986**;147:1283–1287
3. Bellon EM, Haacke EM, Coleman PE, Sacco DC, Steiger DA, Gangarosa RE. MR artifacts: a review. *AJR* **1986**;147:1271–1281
4. Rubin JB, Enzmann DR. Harmonic modulation of proton MR precessional phase by pulsatile motion: origin of spinal CSF flow phenomenon. *AJNR* **1987**;8:307–318
5. Modic MT, Weinstein MA, Pavlicek W, et al. Nuclear magnetic resonance imaging of the spine. *Radiology* **1983**;148:757–762
6. Modic MT, Weinstein MA, Pavlicek W, et al. Magnetic resonance imaging of the cervical spine: technical and clinical observations. *AJNR* **1984**;5:15–22
7. Norman D, Mills CM, Brant-Zawadzki M, Yeates A, Crooks LE, Kaufman L. Magnetic resonance imaging of the spinal cord and canal: potentials and limitations. *AJR* **1983**;141:1147–1152, *AJNR* **1984**;5:9–14
8. Rauschning W, Bergstrom K, Pech P. Correlative craniospinal anatomy studies by computed tomography and cryomicrotomy. *J Comput Assist Tomogr* **1983**;7:9–13
9. Schenck JF, Hart HR, Foster TH, Edelstein WA, Hussain MA. High resolution magnetic resonance imaging using surface coils. In: Kressel HY, ed. *Magnetic resonance annual*. New York: Raven Press, **1986**:151–152
10. Hendrick RE, Kneeland JB, Stark BB. Maximizing signal-to-noise and contrast-to-noise ratios in FLASH imaging. *Magn Reson Imaging* **1987**;5:117–127
11. Niewenhuys R, Voogd J, Huijzen C. *The human central nervous system. A synopsis and atlas*, 2nd rev ed. New York: Springer-Verlag, **1981**:100–107